PHOTOMASK

BACUS—The international technical group of SPIE dedicated to the advancement of photomask technology.

Invited Paper - AL13

Mask effects for high-NA EUV: impact of NA, chief-ray-angle, and reduction ratio

Jens Timo Neumann*, Paul Gräupner, Winfried Kaiser, Reiner Garreis, Carl Zeiss SMT GmbH, Rudolf-Eber-Str. 2, 73447 Oberkochen, Germany

Bernd Geh, Carl Zeiss SMT, c/o ASML-TDC, 8555 S River Pkwy, Tempe, AZ, 85284, USA

ABSTRACT

With higher NA (≫0.33) and increased chief-ray-angles, mask effects will significantly impact the overall scanner performance. We discuss these effects in detail, paying particular attention to the multilayer-absorber interaction, and show that there is a trade-off between image quality and reticle efficiency. We show that these mask effects for high NA can be solved by employing a reduction ratio >4X, and show several options for a high-NA optics. Carefully discussing the feasibility of these options is an important part of defining a high-NA EUV tool.

1. Introduction

EUV lithography is certainly gaining momentum. The NXE:3100 with NA 0.25 has been in the field and working at chip manufacturers' sites for more than a year now; quite a few papers presented at the EUVL symposium 2012 in Brussels showed results obtained with these tools, for an overview of the lithographic performance see, e.g., References.[1,2] The first optics sets for the NXE:3300, "Starlith 3300" with NA 0.33 was shipped from Carl Zeiss to ASML in April 2012, followed by more sets, and several NXE:3300 machines are now being integrated at ASML in the Netherlands and will be shipped to customers starting this year. For an update on the NXE:3300 status, see References[3] (platform) and [4](optics). An impressive resolution capability of 13nm half-pitch for lines and spaces and 18nm half-pitch for contact holes has been shown,[3] see Figure 1. Simultaneously with the completion of the NXE:3300, Carl Zeiss and ASML are looking beyond this tool and are exploring options for EUV tools with even higher resolution, i.e., with higher NA. Feasibility of design solutions

Continues on page 3.

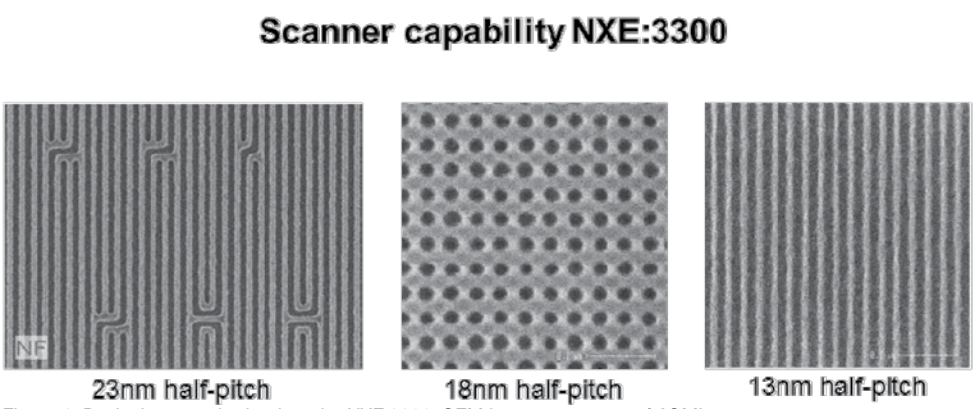

Figure 1. Resist images obtained on the NXE:3300. SEM images courtesy of ASML.

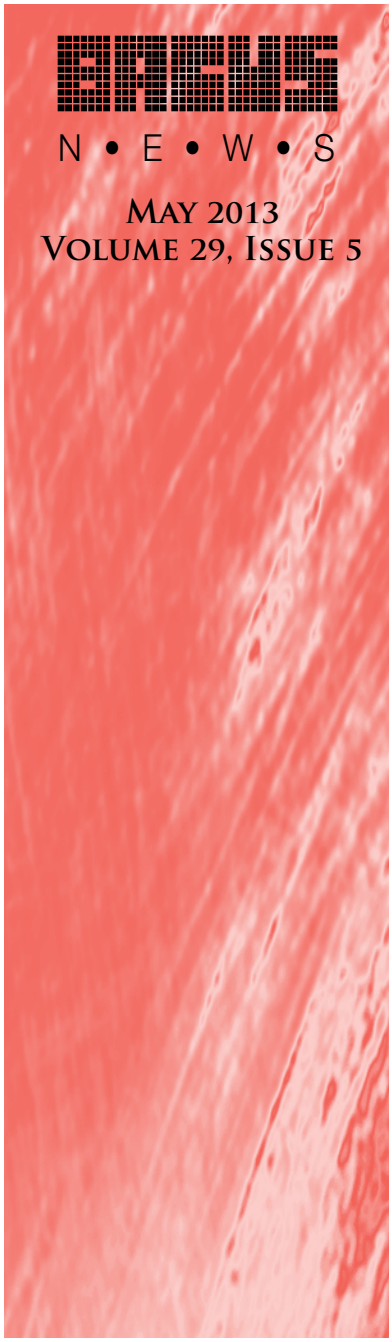

TAKE A LOOK INSIDE:

INDUSTRY BRIEFS
—see page 12

CALENDAR
For a list of meetings
—see page 13

SPIE

8679-40

EDITORIAL

This is not your father's photomask

Tom Faure, IBM Corporation

During a recent discussion with some of my industry colleague's we reflected on how much the photomask has evolved over time and gone from being a simple chrome on glass binary mask with relatively primitive images to what is now essentially a complex optical element in the 193 nm scanner. We agreed that today's mask maker's are being asked to deliver the equivalent of new diffractive optical elements for the most advanced 193 nm scanners on an almost daily basis. How did we get here? Many factors have come into play such as the demise of 157 and the delay in EUV. Regardless of the changes the technology marches forward. With the continued use of 193, immersion, and new illumination schemes, the photomask has been asked to help fill the advanced patterning technology void to try to enable continued scaling of feature sizes . By our own internal accounting at IBM the 10 nm logic node will be our fifth technology generation using ArF immersion lithography. I can remember in the early days of 180 nm node that 193 nm lithography enabled IBM to continue to use the more simple chrome on glass binary masks instead of using the more complex and expensive attenuated phase shift masks at 248 nm.

The industry's extensions of 193 nm immersion lithography for the 10 nm logic node is continuing the trend of forcing more complexity on the photomask. Even the quartz substrate itself has had to come under tighter restrictions in the form of low birefringence and strict flatness specifications. The chrome on glass binary absorber films have been replaced with higher transmission attenuated MoSi films and new/more sophisticated thin binary MoSi films. Hard mask pattern transfer layers have been added to the mask blank film stack to enable resolution of feature sizes as small as 40 nm on the mask. In other words feature sizes on the mask are becoming equivalent to feature sizes on the wafer. This would have been unthinkable only a few years ago. Use of both positive and negative tone chemically amplified resists (CAR) is now the norm versus our previous use of much slower and more stable non-CAR resists. The recent implementation of negative tone develop (NTD) and bright field patterning by optical lithographers for metal and via levels has completely transformed photomasks for these layers from dark field to bright field. Seemingly over night, dark field contact "hole" masks have been converted to bright field contact "dot" masks with new and unique mask manufacturing challenges. The use of so-called "wavefront engineering" approaches such as source mask optimization (SMO) and inverse lithography technology (ILT) that are needed to enable continued extension of 193 nm optical patterning have had a huge impact on photomask complexity. These techniques rely on the photomask to be an integral part of the wavefront engineering solution and require the mask to have billions of complex shapes. Examples of the increasing complexity of mask shapes are shown in the figure below.

As the figure indicates, the increasing photomask shape complexity of advanced SMO and ILT solutions will drive a huge increase in ebeam shot count required to pattern the mask. Classic OPC solutions on a photomask have shot counts of 0.75 Giga shots/cm2 whereas fully aggressive raw ILT solutions have shot counts of 15 Giga shots/cm2. This continuing trend of increasing shot count led to a recent study by Toppan Photomasks to predict ebeam write times of 2-3 days per mask for traditional single beam mask writers!

To make matters worse the defect specifications on the advanced photomasks continue to tighten while mask defect inspection technology struggles to keep up. Defects as small as 30 nm need to be detected on today's advanced photomasks due to the high MEEFs that occur as a result of our efforts to extend 193 nm lithography. However, the complex shapes on our most advanced photomasks make mask defect inspection extremely challenging and require the use of complicated

(continues on page 11)

BACUS N • E • W • S

BACUS News is published monthly by SPIE for BACUS, the international technical group of SPIE dedicated to the advancement of photomask technology.

Managing Editor/Graphics Linda DeLano
Advertising Lara Miles
BACUS Technical Group Manager Pat Wight

SPIE

P.O. Box 10, Bellingham, WA 98227-0010 USA
Tel: +1 360 676 3290
Fax: +1 360 647 1445
www.SPIE.org
help@spie.org

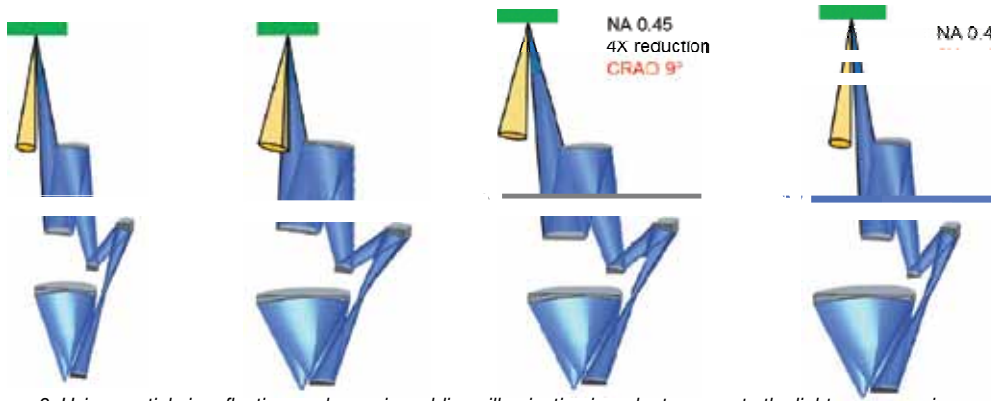

Figure 2. Using a reticle in reflective mode requires oblique illumination in order to separate the light cones coming from the illuminator (from the left, sketched in yellow) and going to the projection optics (sketched in blue) (a). If the NA would be increased without any accompanying measures, these light cones would intersect (b). There are two ways to accommodate for the increased NA and to separate the light cones at the reticle again: One can either increase the chief-ray-angle (c), or adjust the reduction ratio and hence reduce the opening angle of the light cones at the reticle while the NA at wafer, depicted by the wide light cone below the last mirror of the projection optics, remains large (d).

for scanner optics with NA up to 0.7 has been announced in Reference,[5] mentioning for the first time concerns regarding shadowing due to increased chief-ray-angle; also (inorganic) resists have been shown with a resolution of 10nm and below.[6]

These high-NA options have one characteristic which deserves a careful consideration: Since EUV works with reflective masks, the reticle is exposed under oblique incidence in order to separate incident and reflected light. For increased NA, the angles of incidence get larger, and in particular a larger chief-ray-angle is required; these increased angles will have significant impact on image quality, telecentricity, and mask efficiency. Increasing the reduction ratio ("mag") of the projection optics helps to keep incidence angles under control and hence to mitigate or even avoid these mask-induced effects. A better understanding of this interaction between incidence angles, mask effects, and reduction ratio for high-NA EUV lithography is the aim of this paper. A brief introduction to the interaction between NA, chief-ray- angle, and reduction ratio can be found in Section 2. Section 3 gives an account on the relevant mask effects, in particular the interaction between reflective multi-layer and absorber. Various options for dealing with the mask effects are discussed; different ways of multilayer optimization are shown to yield a trade-off between image quality and mask efficiency while an increased reduction ratio yields both, good image quality and high mask efficiency. The simulations used to obtain these results are validated against diffractometry data experimentally obtained at the Lawrence Berkeley National Laboratory (LBNL). Various options for high-NA EUV optics are then outlined in Section 4. Note that all results and conclusions obtained in these sections, in particular the significant benefit of an increased reduction ratio for high-NA EUV, depend on the assumption of using standard mask technology, i.e., a topographic, Ta-based absorber on a reflective multilayer stack. Section 5 briefly comments on the potential of alternative mask concepts. Section 6 finally summarizes the main findings of this paper.

This paper is an extension of the work presented in References.[7,8,9]

2. NA, chief-ray-angle, and reduction ratio

As is well known, EUV lithography uses reflective masks as no transparent materials are available to facilitate a transmission mask. Consequently, the mask has to be exposed with oblique incidence in order to allow for a separation between incident and reflected light, or in other words, between the light cones of illuminator and projection optics, see Figure 2(a). The NXE:3100 with NA = 0.25 and also the NXE:3300 with NA = 0.33 use illumination incident on the mask under a CRAO ("Chief-Ray-Angle-at-Object") of 6°. Now consider the case that the NA, more precisely: the NA at wafer, is increased in order to enhance the resolution capability. For an optics with reduction ratio $\beta = 4$, as is common for today's high-volume lithography, the opening angle of the light cone at the reticle is given by

$$NA_{\text{reticle}} = \frac{NA_{\text{wafer}}}{\beta} = \frac{NA_{\text{wafer}}}{4}. \quad (1)$$

Hence, the opening angle of the light cones at the reticle is growing proportional to the NA at wafer. Consequently, a CRAO of 6° will not be sufficient any more - the light cones of illuminator and PO would intersect, see Figure 2(b). There are two possibilities to separate the light cones again. First, and very obvious, one can just increase the CRAO (Figure 2(c)). Choosing this option, and taking volume constraints for lens manufacturing into account, one would end up with a CRAO of about 9° if aiming at an NA of 0.45. Second, looking at Equation (1), one can increase the reduction ratio β (Figure 2(d)): if, e.g., the NA at wafer is increased from 0.33 to 0.5 (i.e., by a factor of 1.5) and the reduction ratio is increased from $\beta = 4$ to $\beta = 6$ (i.e., also by a factor of 1.5), all angles at the reticle remain unchanged.

3. Mask effect for high-NA

Considering mask effects for high-NA EUV, this section starts with a simplified, geometric sketch of absorber shadowing to illustrate the topic at hand. A quantitative analysis of mask effects is given in Subsection 3.2 in terms of diffraction patterns obtained by rigorous simulations, and the simulations

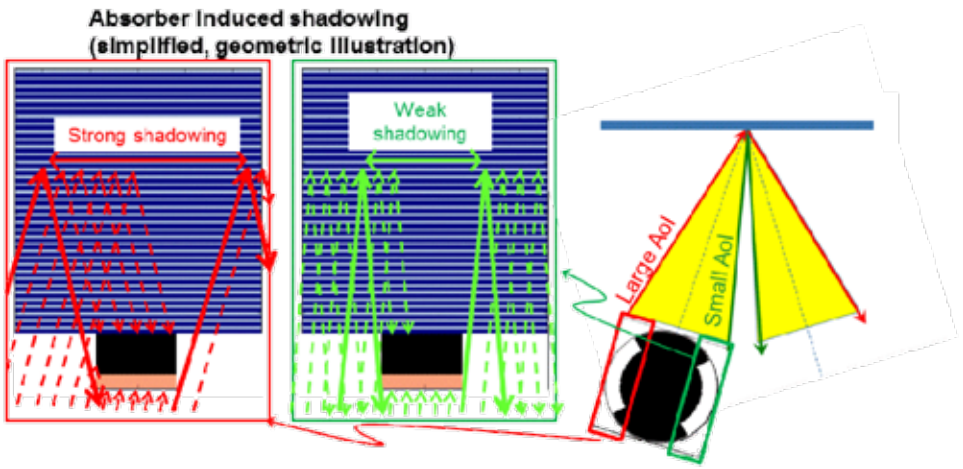

Figure 3. Simplified, geometric sketch of absorber shadowing: There is not just the chief-ray-angle, but a full range of angles incident on the reticle (sketched by the blue bar). Due to the oblique illumination, the angles of incidence are not distributed symmetrically around zero but around the non-zero chief-ray-angle. One pole of the dipole belongs to large angles of incidence and sees a significant shadowing effect while the other pole belongs to small angles and sees a much less pronounced shadowing. In consequence, the two poles see different "effective line widths".

are validated against experimentally obtained diffraction efficiencies. Subsection 3.3 then considers ways to deal with the mask effects and shows that the most promising way is to increase the reduction ratio of the projection optics. This evaluation is done in terms of diffraction patterns as well as in terms of image quality and mask efficiency. Subsection 3.4 then comments on further benefits of an increased reduction ratio. Note that all results and conclusions obtained in this section, in particular the significant benefit of an increased reduction ratio for high-NA EUV, depend on the assumption of using standard mask technology, i.e., a topographic, Ta-based absorber on a reflective multilayer stack.

3.1 Absorber shadowing for high-NA: Qualitative explanation

In order to understand the mask effects on high-NA imaging, it is important to note that there is not only the chief-ray-angle, but there is a whole range of angles incident on the mask. Further, it is important to note that — as an immediate consequence of the non-zero chief-ray-angle — these angles are not distributed symmetrically around zero. As can be seen from the sketch on the right side of Figure 3, one pole of a dipole belongs to small angles of incidence, while the other pole — located at the opposite side of the illuminator NA — belongs to large angles of incidence. Due to this asymmetry, these two poles will experience totally different imaging conditions, as will be outlined in the remainder of this section.

It is well known that the pattern on the reticle is formed by an absorber which is located on top of the reflective multilayer; it is also well known that this absorber casts a shadow, due to its thickness and the oblique incidence of light. It is important to note now that this "shadowing" depends on the angle of the incident light as can be seen in the sketches in Figure 3: Light with a rather shallow angle (left) sees rather strong shadowing and hence sees a relatively wide "effective line width", whereas light with a steeper angle sees a much less severe shadowing and consequently sees a much smaller effective line width. Since we have one side of the illumination pupil — in the example depicted here, one pole of the dipole — at small angles and the other one at large angles, this means that the two poles — more general, the two sides of the illumination pupil — see different absorber shadowing and consequently different effective line widths.

Note that this geometric sketch is a simplification as it neglects, e.g., diffraction effects. Also, the light is not reflected from one clearly defined plane within the multilayer but, due to constructive interference ("Bragg reflection"), from within the bulk of the multilayer; the multilayer behavior can in general be angular dependent and can reinforce or (partially) compensate absorber shadowing. In the next subsection we will show this effect in terms of diffraction patterns obtained by rigorous calculations. However, even the geometric simplification presented in this subsection shows one more thing which is worth noticing: Since light is not reflected from the top of the multilayer but from within it, making the absorber thinner will reduce, but not eliminate the shadowing effect. Even an absorber with zero thickness will cast a shadow to within the multilayer.

3.2 Impact of mask effects on diffraction efficiencies: simulation and experiment

The left part of Figure 4 shows simulated diffraction patterns, for NA 0.33 (CRAO 6°) and for NA 0.45 (CRAO 9°). The upper patterns were obtained for simulated open frame exposures, i.e. no absorber pattern present on the mask. Consequently, the diffraction pattern as it would appear in the pupil plane of the PO contains only 0^{th} order, namely just the illumination dipole as it is reflected from the reticle. We find a well-balanced pattern for the NA 0.33 case, while the NA 0.45 case yields a noticeable difference between the upper pole (small incidence angles) and the lower pole (large incidence angles): The large angles are attenuated by the multilayer stack as the reflectivity of the standard reticle coatings drops for incidence angles $\geq 11°$.

The lower diffraction patterns were obtained for simulated lines-and-spaces exposures, with half-pitch 15nm in the NA

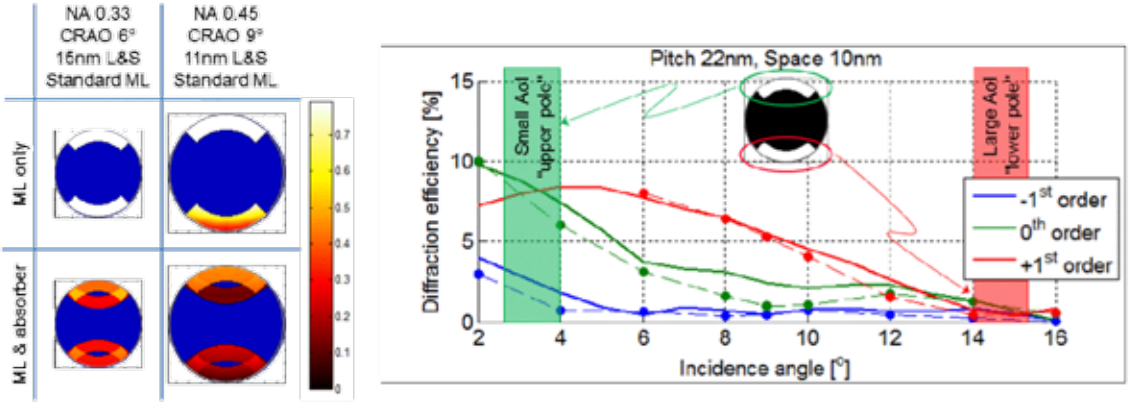

Figure 4. Left part: simulated diffraction patterns for NA 0.33, CRAO 6°, and for NA 0.45, CRAO 9°. In the NA 0.45 case, mask effects (multilayer apodization and absorber shadowing) induce clearly visible asymmetries. Right part: Diffraction efficiencies measured at Lawrence Berkeley National Lab (dots), and simulated with the mask stack used throughout this paper (thick lines). Even though the simulation stack was not optimized to match the experiment, a nice agreement is found between simulation and experiment.

0.33 case and 11nm in the NA 0.45 case. Looking closely, one can find some absorber shadowing even in the NA 0.33 case: The 0th order of the lower pole (large incidence angles) is a little attenuated compared to the upper pole. In the next section we will present some imaging data and show that this shadowing effect for NA 0.33 is tolerable. For the NA 0.45 case, however, the imbalance between the two poles of the dipole is much more severe: as expected from the simple geometric consideration presented in the preceding section, the absorber induces significant shadowing on the lower pole (large incidence angles) and far less shadowing on the upper pole. Consequently, the lower pole is much more attenuated compared to the upper pole than in the NA 0.33 case. The multilayer apodization, which also attenuates the lower pole, reinforces this effect. This asymmetry of 0th orders will lead to noticeable telecentricity effects as has been noted, e.g., in References.[10,11] Apart from this imbalance of 0th orders, it can further be seen that the 1st diffraction order of the upper pole also is much weaker than the 0th order. This is plausible if one takes into account that this 1st order is diffracted into a large angle of exit from the reticle and hence is shadowed by the absorber. Such an intensity imbalance between 0th and 1st order will lead to inconvenient contrast loss in the aerial image. This effect has been noted in Reference,[12] but generally it appears to be far less well known than the telecentricity effect; as this contrast loss effect, however, clearly is of great importance we will focus on this effect in the subsequent subsection. Some remarks on mask induced telecentricity, and the possibility of correcting for it by means of illumination, can be found in the appendix of Reference.[8]

In order to validate the simulations on mask effects for high-NA imaging, diffractometric experiments were done at the Lawrence Berkeley National Lab using a reticle manufactured by Samsung; a detailed account on these experiments, and on deriving calibrated models of the mask stack for simulational use, can be found in reference.[13] The results of one of these measurements are shown in the right part of Figure 4; the dots give the measured diffraction efficiencies as a function of the incidence angle, the lines give efficiencies simulated with the mask stack used for all simulations in this paper. Although the simulations were done prior to the experiment, and hence the mask stack was not optimized to match the experiment, there is a very nice agreement between the simulation and the experiment.

3.3 Dealing with mask effects: multilayer tuning vs. increased reduction ratio

The previous subsection investigated mask effects in terms of diffraction patterns, showing in rigorous simulations and in experiments the asymmetries expected from the simplified geometric sketch outlined in Subsection 3.1. The present section will again employ rigorous simulations, and will apply these simulations to three possible strategies to cope with the mask effects at high-NA imaging. The first two options are given by two different optimizations of the multilayer stack. One multilayer is optimized for broadband reflectivity, as can be seen in the open frame pattern (upper row) of the third column of Figure 5: With this multilayer stack, both poles are reflected with the same efficiency in spite of their different angles of incidence. The full diffraction pattern including absorber, however, still yields a noticeable asymmetry (lower row) since the absorber, as argued before, attenuates the large angles of incidence. The second option uses a multilayer stack which is optimized for the specific use case at hand as can be seen in the fourth column of Figure 5: While the open frame reflectivity (upper row) shows a significant imbalance, viz. an attenuation of the upper pole (small angles of incidence), the full diffraction pattern with absorber (lower row) is well balanced; this can be understood since the absorber, as before, attenuates the large angles of incidence which is exactly opposite to the multilayer behavior. However, this mutual attenuation of small and large incidence angles by multilayer and absorber of course comes at the loss of mask reflectivity. The third option is different from the first two options as it still uses the standard reticle stack. Instead of tuning the mask, now the reduction ratio is used to accom-

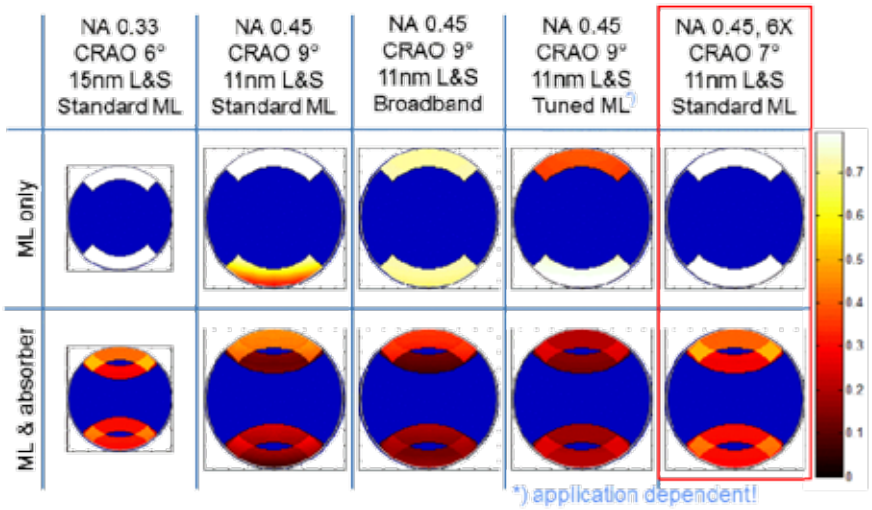

Figure 5. Diffraction patterns simulated for open frame exposure (pure multilayer reflection) and for lines&spaces with k_1 = 0.37. It is clearly seen that the standard multilayer, when used with NA 0.45, CRAO 9° to expose 11nm dense lines and spaces, yields asymmetric diffraction patterns, both open frame and with absorber (second column). Using a broadband multilayer helps to obtain a symmetric open-frame reflection, but the angular dependent absorber shadowing discussed in the text still yields an asymmetric diffraction pattern if the absorber is present on the mask (third column). It is possible to tune the multilayer such that the effects of multilayer and absorber compensate (fourth row): the multilayer attenuates the small angles of incidence, and the combined multilayer and absorber effects then yield a rather symmetric diffraction pattern. However, this compensation comes at a general loss of reticle reflectivity. Using the standard multilayer, but increasing the reduction ratio 6 helps a lot since it reduces the incidence angles at the reticle while maintaining the high NA at the wafer: The diffraction patterns, both multilayer only and with absorber, are symmetric as in the NA 0.33 case but now with a resolution of 11nm half-pitch instead of 15nm.

modate for the high NA. As can be seen in the last column of Figure 5, the diffraction pattern, both open frame and with absorber, look very much like in the NA 0.33 case, but now at a finer resolution of 11nm half-pitch instead of 15nm. This is very plausible: we still have a high NA at wafer, indicated by the wide radius of the diffraction pattern in this figure; by means of the increased reduction ratio, however, we can reduce the NA at reticle to a value which, for this example, is even below the NA 0.33 case. By Equation (1), we have $NA_{\text{reticle}} = \frac{0.33}{4} = 0.0825$ in the NA 0.33 case, and $NA_{\text{reticle}} = \frac{0.45}{6} = 0.075$ in the NA 0.45 case with reduction ratio 6. Hence, all mask effects are even reduced compared to the NA 0.33 case in spite of the increased NA at wafer, and this allows for fine resolution at wafer without suffering from mask effects.

Now we take it one step further and calculate imaging properties; in particular, we will look at image quality, represented by the image contrast, and the relative mask reflectivity. Figure 6 shows the results of these simulations; the blue bars represent the contrast of the aerial image, the red bars represent the mask reflectivity normalized to the reflectivity obtained for the NA 0.33 case. It is clearly seen that with the standard multilayer, both image contrast and mask reflectivity drop for the NA 0.45 case as compared to the NA 0.33 case, although the half-pitch has been scaled such that in both cases we have k_1 = 0.37 and hence would naively expect a similar performance. The difference between these two cases is, of course, given by the large incidence angles at the reticle in the NA 0.4 case. A broadband multilayer which ensures a uniform reflectivity of the multilayer throughout the whole range of incidence angles helps to improve contrast as well as mask efficiency but still stays short of the performance of the NA 0.33 reference case.

The tuned multilayer compensates for the angular dependent absorber shadowing by attenuating the small incidence angels and indeed helps to further improve the image contrast, but this gain in contrast comes at the loss of mask efficiency as outlined above. The increased reduction ratio, however, regains the performance of the NA 0.33 reference case in both image contrast and mask efficiency, but now at a resolution of 11nm half-pitch as compared to 15nm half-pitch in the NA 0.33 case. These results confirm the observations made in the preceding paragraphs: At high NA, and staying with a reduction ratio 4X, mask effects will have noticeable impact on the reticle performance in terms of image quality and mask efficiency. Adopting the reduction ratio enables to maintain the large NA at wafer, at hence enable a fine resolution, while not suffering from mask effects since the incidence angles at the reticle remain relatively low.

A corresponding result can also be obtained for contact holes, as summarized in Figure 7. Again, we start by simulating a reference case, 19nm dense contact holes at NA 0.33, CRAO 6°. We find a NILS ("normalized image log slope") of 2.5; as a rule of thumb, NILS should be above 2 for a reasonable process, so we are well above this requirement. As before, we set the mask reflectivity, or mask efficiency, obtained in this reference case to 100%. Then we look at 14nm dense contact holes at NA 0.45 and CRAO 9°; as in the previous example, k_1 is identical for the NA 0.33 and the NA 0.45 case. For the NA 0.45 case, we show the results obtained with a multilayer optimized to compensate for the angular dependent absorber shadowing, and we find that this is sufficient to get a NILS of 2 (right group of bars in the left plot of Figure 8), but we have

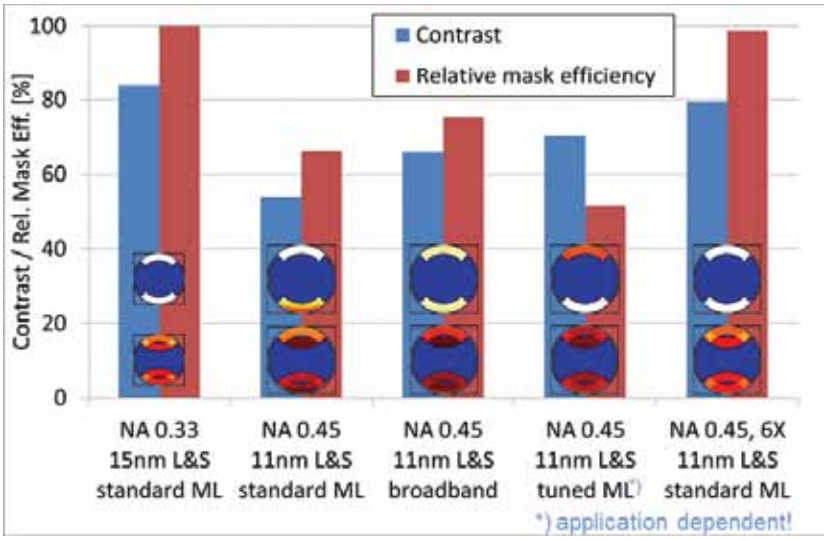

Figure 6. Image quality, represented by the image contrast, and mask efficiency, normalized to the NA 0.33 reference case, for various options at NA 0.45. At high NA, and staying with a reduction ratio 4X, mask effects will have noticeable impact on the reticle performance in terms of image quality and mask efficiency. A broadband multilayer with uniform reflectivity over the whole range of incidence angles helps somewhat but still stays short of image contrast and mask efficiency obtained in the NA 0.33 reference case. Further tuning the multilayer to compensate for the angular dependent absorber shadowing further improves the image contrast, but only at the loss of mask efficiency. Adopting the reduction ratio, however, enables to maintain the large NA at wafer, and hence enables a fine resolution, while not suffering from mask effects since the incidence angles at the reticle remain relatively low. Hence, the performance of the NA 0.33 reference case is achieved in both image contrast and mask efficiency, but now at resolution of 11nm half-pitch instead of 15nm.

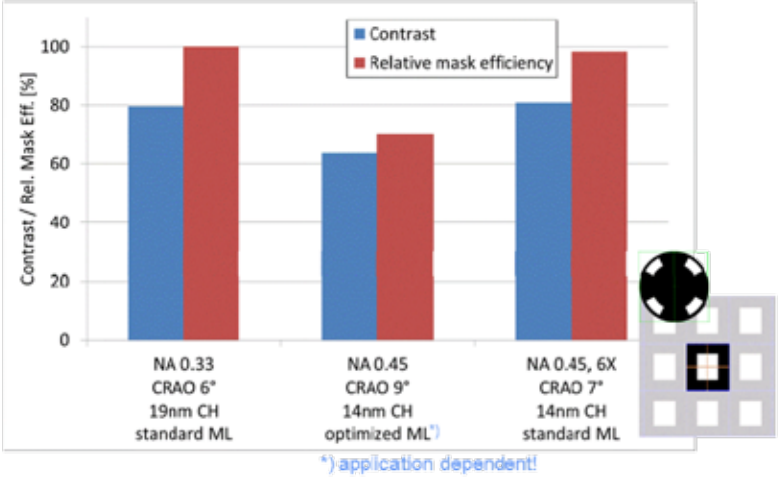

Figure 7. Image contrast of the aerial image and relative mask efficiency for dense contact holes. NA 0.33, CRAO 6° gives a good performance for 19nm half pitch (left group of bars), with the standard multilayer. NA 0.45, CRAO 9° achieves a contrast of 64% (about the minimum required for reasonable process latitude) for 14nm half pitch with a multilayer optimized to compensate for the angular dependent absorber shadowing (center group of bars). The relative mask efficiency, however, then drops to ~70% of the efficiency in the NA 0.33 case. Adjusting the reduction ratio (here: NA 0.45 with reduction ratio 6X and CRAO 7°) helps to recover both good image contrast and mask efficiency with the standard multilayer (right group of bars).

a loss of mask efficiency of ~30% as compared to the reference case (right bar in the right plot). Changing the reduction ratio helps also in this case: With NA 0.45, reduction ratio 6X, and CRAO 7° (and the standard multilayer stack) we find back the image quality as well as the mask efficiency we had in our reference case (indicated by the shaded areas in the graphs of Figure 8), but now at a resolution of 14nm dense contact holes.

3.4 Benefits of increased reduction ratio for mask making

The previous subsection showed how an increased reduction ratio helps to simultaneously get good image quality and good mask efficiency for high-NA EUV. The root cause is, of course, that an increased reduction ratio helps to keep incidence angles at the reticle on a similar level as in NXE:3300, and hence keep

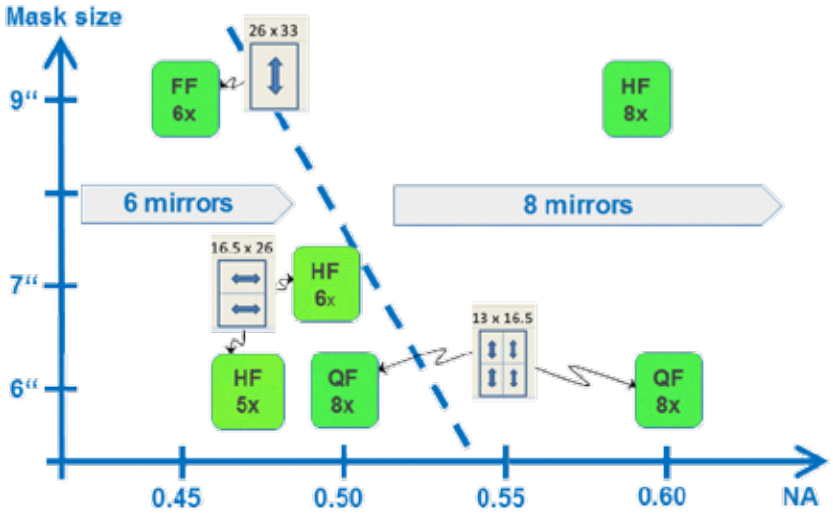

Figure 8. Options for high-NA EUV optics, described by NA (x-axis), reticle size (y-axis), reduction ratio, wafer field size: full-field ("FF", 26x33mm²), half-field ("HF", 16.5x26mm²), and quarter-field ("QF", 13x26mm²), and number of mirrors in the projection optics (with the dashed line indicating the approximate regimes of the six mirror ("6M") and eight mirror ("8M") options.

mask induced effects under control. Note that the good performance shown in the preceding subsection was obtained with a standard reticle stack as expected to be used on NXE:3300. This is a huge benefit compared to the option "mag 4X, CRAO 9°, tuned multilayer" which was also discussed: In addition to the trade-off between image quality and mask efficiency which was found in the previous subsection, the multilayer tuning depends on the details of mask pattern and illumination setting, and hence this approach would require a library of tuned multilayers for different use cases which would be disadvantageous from a logistics point of view and would also require stable manufacturing processes for various, maybe even setting dependent multilayer stacks.

There is yet another benefit of the increased reduction ratio for high-NA EUV which was not part of the discussion in the preceding subsections but can hardly be overestimated, and this is related to the requirements towards mask making. Dense lines with half-pitch 13nm line at wafer, which is about the limit to be printed with NA 0.33 and 4X reduction ratio (k_1 = 0.318), would correspond to 52nm half-pitch at reticle. Now consider a sub-10nm half-pitch at wafer, say, e.g., 8.5nm half-pitch. Printed with NA 0.5, this would result in k_1 = 0.315 and hence is rather comparable to the 13nm at NA 0.33 (provided one has found a way to deal with the mask effects outlined above). Of course, staying with reduction ratio 4X, this would correspond to a 34nm half-pitch at the reticle, i.e., a shrink by a factor of 0.65 compared to the 52nm mentioned above. All requirements to mask making, like linearity, CD control, placement, etc., would scale accordingly; further, admissible defect sizes would shrink as well. This would make it significantly more difficult than today to facilitate an acceptable mask and, according to the ITRS roadmap, no solutions are visible for masks to be used on lithography tools with NA beyond 0.33, see Reference.[14]

If, however, the NA 0.5 comes with a reduction ratio of, e.g., 8X, then the 8.5nm half-pitch at wafer corresponds to 68nm half-pitch at reticle, which is even relaxed as compared to the 52nm mentioned above. Remember that we originally proposed the increased reduction ratio for high-NA EUV in order to cope with mask effects associated with the incidence angles at mask (which also apply to a perfectly manufactured mask). As a side effect, however, this means that features on the mask will not shrink compared to NXE:3300 applications (shrink at wafer, however, will be enabled by the increased reduction ratio), and hence the requirements to mask manufacturing will not tighten as strictly as they would do for high-NA EUV with 4X reduction ratio, making it much more likely to manufacture an acceptable mask with reasonable effort.

4. Exposure tools: options for high-NA EUV

There is a wide range of options available for a high-NA EUV system, as is sketched in Figure 8. In this graph, the options are sorted by NA (x-axis) and reticle size (y-axis). It is evident that a modified reduction ratio will have impact on the relation between reticle size and field size at wafer. On a system with reduction ratio 4X, the current die size at wafer, 26x33mm², translates into 104x132mm² at the reticle, and this fits well into a 6" reticle (6" = 152.4mm, i.e., there remain 20.4mm margin for manufacturing (edge) effects, markers, etc.). To get this 26x33mm² wafer field on a system with reduction ratio 6X, one would need a 9" reticle instead. Given the effort which would be required to move to reticle sizes different from 6", however, most options depicted in Figure 8 do indeed use a 6" reticle. One could, e.g., choose a reduction ratio of 5X and go for a half-field on the wafer: The die size would then be 16.5x26mm (so two of these dies would add up to the current 26x33mm² die), and the long side of this half-field would again fit well into a 6" reticle (26mm @ wafer → 130mm @ reticle, so there are >20mm margin). Aiming at incidence angles at reticle comparable to NXE:3300, $NA_{reticle} = \frac{0.33}{4} = 0.0825$, one could choose NA 0.45 for either option of these two: then, the first option

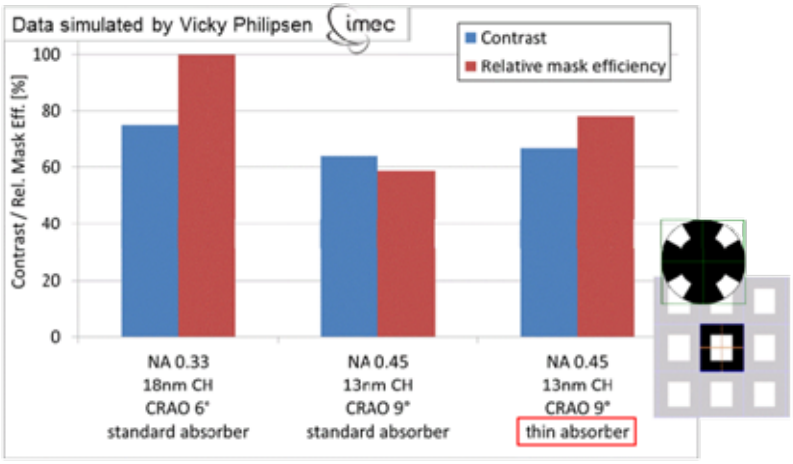

Figure 9. Image contrast and relative mask efficiency obtained by Vicky Philipsen (IMEC) for regular grids of dense contacts for various NAs (all with a reduction ratio of 4X), with a standard, Ta-based absorber of 51nm thickness and a theoretical, more opaque absorber material of only 26nm thickness. The half-pitch is chosen such that k_1 is approximately constant for both NA options (k_1 = 0.43 … 0.44). For the NA 0.45 cases, an application specific, optimized multilayer is used. The contrast loss due to mask effects at high-NA is comparable for both absorbers, but the thin absorber significantly helps to reduce the loss of relative mask efficiency. However, even with the thin absorber ≥20% loss of mask efficiency is observed.

(full field with reduction ratio 6X, 9" reticle) would come with $NA_{reticle}$ = 0.075 and the latter option (half field with reduction ratio 5X, 6" reticle) with $NA_{reticle}$ = 0.09. If one is willing to accept some amount of mask effects, the NA for the half-field option could be extended to NA 0.5 (i.e., $NA_{reticle}$ = 0.1): considering the incidence angles at the reticle, this would somewhere in between the NXE:3300 and the NA 0.45 with reduction ratio 4X considered in the previous section ($NA_{reticle}$ = 0.1125). Hence, mask effects would be somewhat visible but less severe than those shown in Section 3. The charm of this option is then that it combines the high NA of 0.5 with the half field while still using a 6" reticle. Working with a quarter-field, however, would allow for this high NA of 0.5 while keeping the incidence angles at the reticle even below those of the NXE:3300: going for a reduction ratio 8X, the quarter field (13x16.5mm^2) would translate into the familiar 104x132mm^2 field at reticle, and the NA at reticle would be reduced to $NA_{reticle}$ = 0.065. At the expense of reduced field size, this option combines the resolution capabilities of the high NA 0.5 with freedom from mask effects, while maintaining the 6" reticle. From a pure mask related point of view, one could even increase the NA of this quarter-field option to NA 0.6 ($NA_{reticle}$ = 0.075), probably requiring another two mirrors in the projection optics in order to obtain a decent wave front correction.

Design options for the projection optics are available for the NA / reduction ratio / field size combinations outlined above; all these options will have a central obscuration which helps to limit the angular spread on the mirrors of the projection optics. These options differ not only in NA (and hence resolution) and reduction ratio (and hence field or reticle size) but also in transmission (and hence throughput): Based on current design studies, the options with NA ≤ 0.5 come with a transmission comparable to NXE:3300; pushing the NA to 0.6 would require two additional mirrors which would reduce the transmission to ~40% of NXE:3300. To make a proper trade-off between field size, NA, and transmission, is work in progress.

Summarizing these briefly sketched considerations, there are various options available to extend the NA beyond the NA 0.33 of the NXE:3300. The task now is to carefully consider, evaluate, and discuss the advantages and possible drawbacks of the numerous available options and then make the right choice.

5. Comment on the potential of alternative mask stacks

As indicated before, the results and conclusions derived in the preceding section depend on the assumption of current mask technology, i.e., a topographic, Ta-based absorber on a reflective multilayer stack. In particular, the finding that an increased reduction ratio of 5X, 6X, or even 8X would be highly beneficial for high-NA EUV depended on the requirement that incidence angles on the reticle need to be under control. If a mask concept would be available that could handle large incidence angles without causing, e.g., contrast loss or a drop in mask efficiency as outlined in the preceding sections, a reduction ratio of 4X would again be a relevant option for high-NA EUV, and could be supported by the projection optics design. We briefly comment on two possible options: a hypothetical new absorber material which would allow for a thinner absorber for a binary mask, and the potential of phase shifting masks. This is meant merely as an outlook to what could be possible. More extensive simulation results can be found in Reference[15] for the thin absorber, and in Reference[16] for the phase shifting mask. The feasibility of all concepts mentioned here is still open.

5.1 Binary mask with new, extremely thin absorber material

The simplified sketch of angular dependent absorber shadowing in Section 2 suggests that the absorber shadowing effect could be reduced if the thickness of the absorber could be reduced. (Note, however, that one cannot expect to fully eliminate absorber shadowing, even with an absorber of "zero"

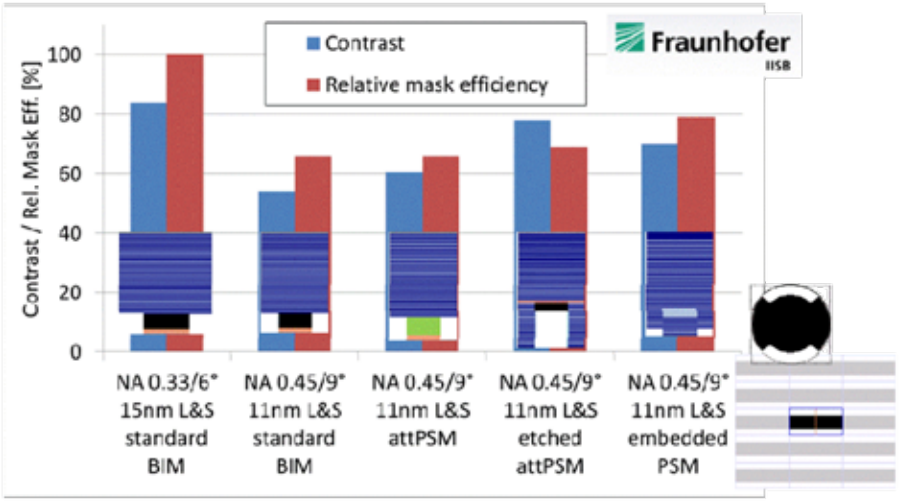

Figure 10. Image contrast and relative mask efficiencies obtained by Andreas Erdmann for 11nm dense lines and spaces, for different mask concepts. For comparison, the standard binary mask with a Ta-based absorber is included (leftmost group of bars). An attenuated phase shifting mask (attPSM, second group of bars), which uses a TiN-/TaNbased absorber, yields roughly the same performance as the standard binary mask. The etched PSM (third group of bars), however, is able to improve the contrast without sacrificing mask efficiency. The embedded PSM finally, whicheffectively is a kind of high-reflection phase shifter mask, yields an image contrast lower than the etched attPSM but still higher than the standard binary mask, and increases the relative mask efficiency.

thickness, as the reflection is from the bulk of the multilayer stack rather than from its surface.) The current, Ta-based absorber is typically used with thicknesses between 50nm and 75nm. It has been shown that it is hardly possible to reduce the thickness of the Ta-based absorber to below 50nm as too much light will "leak" through such a thin absorber which again results in a deteriorated image contrast;[17] instead a new, more opaque absorber will be needed. A theoretical candidate for such a material has recently been investigated by Vicky Philipsen from IMEC;[15] some results obtained in that study are reproduced in Figure 9.

Figure 9 compares simulation results obtained for a standard, Ta-based absorber with 51nm thickness and a hypothetical new absorber material of only 26nm thickness. As before, we use image contrast and relative mask efficiency as figures of merit. A regular grid of dense contact holes, exposed with a quasar-type illumination, was chosen for this simulation study. The left most group of bars gives the results obtained for an NA 0.33 case, with a contact half pitch of 18nm (k_1 = 0.44). The two right groups of bars then give the results found for 13nm contact half pitch, exposed with NA 0.45 (k_1 = 0.43) and CRAO 9°. With an application specific multilayer optimization, an image contrast of 63~67% can be maintained in spite of increasing incidence angles at the reticle. The mask efficiency, however, drops to about 60% for the standard absorber; also the new, thin absorber cannot recover the full mask efficiency of the NA 0.33 reference case but only 85%, which at least is a significant improvement as compared to the standard absorber. We conclude that the thin absorber has the potential to partially mitigate, albeit not eliminate, mask effects for high NA.

5.2 Phase-shifting masks

Another possibility for alternative mask concepts would be to move away from the binary mask and have a look at phase shifting masks. This appears to be promising as, simply speaking, the absorber then doesn't need to be "really dark" and hence one can hope for reduced shadowing. Three concepts for phase-shifting masks have recently been investigated by the Andreas Erdmann et al., see Reference.[16] Sketches of the considered mask concepts are included in Figure 10. The first concept considered there was a high-reflection phase shifter mask which uses an embedded, patterned Molybdenum-layer as phase shift layer. The other two options were attenuated phase shifter masks. One approach looks very much like a standard, binary mask but uses a TiN/TaN-absorber with rather low absorption instead of the usual Tabased absorber.[18,19,20] The other approach controls the phase of the reflected light by etching into the multilayer (hence, we call this an "etched attPSM") and uses a thin absorber layer to control the reflectivity.[18,19,21]

Some of the simulation results obtained by Andreas Erdmann are reproduced in Figure 10. Again, we use the image contrast and the relative mask efficiency as figures of merit. It turns out that the attPSM with the TiN/TaNabsorber (second group of bars) behaves very much like the standard binary mask with the Ta-based absorber (left most group of bars). The etched PSM (third group of bars), however, gives a significant gain in image contrast (78% compared to 54% for the binary mask) while maintaining the mask efficiency obtained for the binary mask. The embedded PSM finally (rightmost group of bars) yields an image contrast of 70%, i.e., somewhat lower than the etched PSM but still higher than the binary mask, and features a 20% improvement in mask efficiency as compared to the binary mask. Similar to the preceding subsection, we conclude that the etched attPSM and the embedded phase shifting mask have the potential to mitigate, albeit not eliminate, mask effects for high NA.

We note that the results presented in this section are purely based on simulations. An experimental evaluation of the

presented mask concepts, assessing key questions like, e.g., manufacturability was beyond the scope of the present analysis and has still to be done.

6. Conclusion

We have investigated mask effects for high-NA EUV, and have shown that the mask effects can be brought under control if one increases the reduction ratio; this helps to maintain relatively small incidence angles at the reticle while the NA at wafer can become large to enable a fine resolution. We conclude that high-NA EUV is feasible from an optical point of view. Indeed, design options for the optics are available, e.g., for a system with NA 0.5 and a reduction ratio 8X, exposing a quarter field (13x16.5mm^2). Such a system would combine the benefit of high-NA with the freedom from mask effects, and would still employ the familiar 6"-reticles. Of course, with larger reticles, larger fields would be possible.

It is in fact the 3D-mask effects which force the optics towards an increased reduction ratio. Current mask technology is likely to be limited to >50nm half-pitch at mask (~13nm half-pitch at wafer, 4X). Further shrink at wafer can then be realized by the high-NA and increased reduction ratio. As a side effect, the increased reduction ratio will help to ease the requirements towards mask making.

We further reported some simulation results which show that alternative mask concepts (thin absorber, PSM) have some potential to mitigate, albeit not eliminate, mask effects for high NA. Until now, these findings are based purely on simulations, and any interest in further evaluating one of the mentioned concepts (or yet another promising candidate) is welcome.

7. Acknowledgments

The authors thank Seong-Sue Kim (Samsung), Harry Levinson and Obert Wood (Global Foundries), Vicky Philipsen, Eric Hendrickx, and Rik Jonckheere (IMEC), Patrick Naulleau, Eric Gullikson, and Rick Chao (LBNL), Natalia Davydova, Steve Hansen, Rudy Peters, and Bill Arnold (ASML), Andreas Erdmann (Fraunhofer Institute), and Johannes Ruoff (Carl Zeiss SMT) for valuable input, discussions, and support.

8. References

[1] van Setten, E. et al., "NXE:3100, getting to know the secrets of EUV Lithography," International Symposium on Extreme Ultraviolet Lithography, Brussels (2012).

[2] Hendrickx, E., "ASML NXE:3100 pre-production EUV scanner performance at IMEC," International Symposium on Extreme Ultraviolet Lithography, Brussels (2012).

[3] Peters, R. et al., "ASML's NXE platform performance and volume introduction," **Proc. SPIE 8679,** 8679-50 (2013).

[4] Lowisch, M. et al., "Optics for ASML's NXE:3300 platform," **Proc. SPIE 8679,** 8679-52 (2013).

[5] Kaiser, W. et al., "The future of EUVL," **SPIE 6924** (2008).

[6] Ekinci, Y. et al, "Evaluation of resist performance with EUV interference lithography for sub-22-nm patterning," **Proc. SPIE 8322,** 83220W (2012).

[7] Kaiser, W., SEMATECH Litho-Forum, Vancouver (2012).

[8] Neumann, J.T., Gräupner, P., Kaiser, W., Garreis, R., Geh, B., "Interaction of 3D mask effects and NA in EUV lithography," **Proc. SPIE 8522,** 852211 (2012).

[9] Neumann, J.T., Gräupner, P., Ruoff, J., Kaiser, W., Garreis, R., Geh, B., "3D reticle effects for high NA EUV lithography," International Symposium on Extreme Ultraviolet Lithography, Brussels (2012).

[10] Philipsen, V. et al., "Impact of mask stack on high-NA EUV imaging," International Symposium on Extreme Ultraviolet Lithography, Brussels (2012).

[11] Ruoff, J., "Impact of mask topography and multilayer stack on high NA imaging of EUV masks," **Proc. SPIE 7823,** 78231N (2010).

[12] Cho, H.-K., "EUV readiness and EUV PPT performance," International Symposia on Extreme Ultraviolet Lithography and Lithography Extensions, Miami (2011).

[13] Chao, R. et al., "Experimental verification of EUV mask limitations at high-numerical apertures," **Proc. SPIE 8679,** 8679-57 (2013).

[14] ITRS Roadmap, http://www.itrs.net/.

[15] Philipsen, V. et al., "Mask stacks for EUV imaging at high NA," IMEC PTW October 2012, Leuven (2012).

[16] Erdmann, A. et al., "Modeling studies on alternative EUV mask concepts for higher NA," **Proc. SPIE 8679,** 8679-61 (2013).

[17] Davydova, N. et al., "Imaging performance improvements by EUV mask stack optimization," **Proc. SPIE 7985,** 79850X (2011).

[18] Han, S.I. et al., "Development of phase shift masks for extreme ultraviolet lithography and optical evaluation of phase shift materials," **Proc. SPIE 5374,** 261 (2004).

[19] Constancias, C., "Phase shift masks for EUV lithography," **Proc. SPIE 6151** [61511W] (2006).

[20] Yan, P. et al., "Extreme ultraviolet embedded phase shift mask," J. Micro/Nanolith., MEMs, MOEMs 10, 033011 (2011).

[21] la Fontaine, B. et al., "Demonstration of phase shift masks for extreme-ultraviolet lithography," **Proc. SPIE 6151,** 61510A (2006).

EDITORIAL

(continued from page 2)

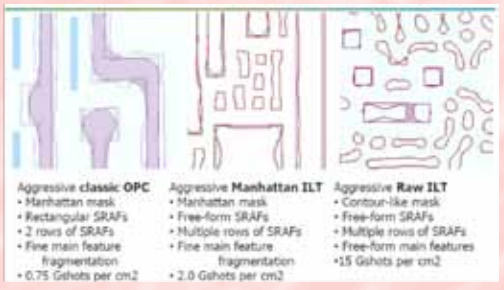

Courtesy Mentor Graphics Corp.

inspection recipes and rules to "ignore" the nuisance detections. In addition, our photomask AIMS defect analysis tools need to be capable of emulating the ever increasing number of complex pixilated scanner sources that are being used for exposing each different photomask.

To paraphrase the words of a famous automobile commercial, "No this is definitely not your father's photomask." As mask makers and lithographers, it is absolutely critical that we work together to try to achieve reasonable solutions to extend optical patterning that all interested parties can live with while at the same time work to address the inadequacies of EUV lithography for the good of the industry. No one company can do it alone. Support and coordinated efforts from mask equipment makers, OPC and design software companies, scanner companies, materials suppliers, mask makers, lithographers, and chip designers are needed to overcome the patterning challenges. As the largest mask conference in the world, the 2013 SPIE Photomask Conference (aka BACUS) to be held September 10-13 provides an excellent forum for discussing and addressing these challenges.

Industry Briefs

Intel Takes On Chip-Production King Taiwan Semiconductor

By **Bruce Einhorn, Ian King, and Tim Culpan**

Like most Silicon Valley chip-design specialists, Altera has long adhered to a trusted formula: Design semiconductors at home; produce them in Asia. For the San Jose based company, which sells phone-equipment processors, that's meant outsourcing production to TSMC, whose cutting-edge chipmaking plants save customers the $4 billion or more it'd cost to build their own. TSMC is the leader in the $39.3 billion contract (foundry) manufacturing industry for chips—taking roughly $7 per smartphone sold. In late February, though, Altera announced that it's taking its advanced chip orders to Intel, which has traditionally focused on making its own microprocessors rather than producing those of other firms. With PC sales in the doldrums, the world's biggest chipmaker needs to find new uses for its excess production capacity. Winning business from Altera "is a huge confidence boost for our team," says Sunit Rikhi, Intel's vice president in charge of its foundry business. Intel has also signed up as clients smaller designers such as Tabula and Achronix Semiconductor. And it will produce chips for Cisco Systems, say two people with knowledge of the matter who aren't authorized to discuss it publicly. Those wins are just warm-ups as Intel battles TSMC and other foundries for a much bigger prize: Apple. The iPhone maker spent $3.9 billion last year on custom chips from Samsung, according to data from IC Insights, and wants to diversify its chip sources to avoid enriching its archrival, says Steven Pelayo, an analyst with HSBC in Hong Kong.

With the competition among the chipmakers heating up, it's unclear how many other new customers Intel can grab. Many larger semiconductor designers that don't compete with TSMC do compete with Intel for design contracts, and that limits the field for the Santa Clara (Calif.)-based chipmaker. "I wouldn't expect Nvidia (NVDA) or Qualcomm (QCOM) or Broadcom (BRCM) to be looking for an opportunity to get in bed with Intel," says Steve Myers, an analyst in Tokyo with Ji Asia. "A large part of the TSMC customer base isn't necessarily going to be interested in Intel."

Intel, Samsung to Dominate Chip Capex in 2013

By **Peter Clarke**

LONDON – Intel and Samsung will spend $25 billion on increasing their manufacturing capacity in 2013 as this sector of the industry continues to consolidate round very few leading-edge manufacturers, according to IC Insights.

Five companies that are expected to spend at least $3.0 billion in 2013, the same as in 2012 and 2011 and the top-10 capital spenders in 2013 are forecast to increase their spending by 5 percent as compared to 2012, while non-top-10 companies are expected to cut spending by 8 percent.

Over the four-year period 2010 to 2013 Samsung is forecast to spend $46.9 billion, with about 60 percent on its memory production and 40 percent on its break into logic and foundry services. Over the same period Intel is forecast to make $40.0 billion in capital expenditure. "Notably, the combined spending by Samsung and Intel represented 40 percent of the world's semiconductor capital outlays in 2012, with this percentage expected to rise to 42 percent of total capital spending in 2013," IC Insights observed.

IC Insights has also broken the forecast data down by geography. This reveals that, thanks to Intel and Samsung, North America and Korea are of growing significance in chip manufacturing. Japan with 7 percent and Europe with 2 percent of expected capex are more or less out of consideration. Europe's very low figure reflects the almost complete adoption of a fab-lite strategy across the continent.

Taiwan's flat share is due to the second-tier DRAM producers Nanya, Powerchip and ProMOS keeping capex to a minimum while foundries TSMC and UMC strive to be aggressive, IC Insights said.

TSMC Expected to Begin 20-nm Line Early

LONDON – Foundry Taiwan Semiconductor Manufacturing Co. Ltd. (Hsinchu, Taiwan) is reportedly going to start installing equipment for 20-nm CMOS production at its Fab 14 on April 20, two months earlier than previously planned.

TSMC would then be able to begin volume production at the end of the second quarter and ramp 20-nm production in the second half of 2013 a Focus Taiwan report said referencing unnamed sources.

That timetable seems extreme as it usually takes several months to get a production line hooked up and another few months for the first wafers to "pipeclean" the line. However a smooth installation could get some additional 20-nm production out in 2013.

At a groundbreaking ceremony for phase 5 of Fab 14 held in April 2012 TSMC indicated that the fab would be TSMC's second 20nm-capable fab area and planned to begin 20-nm volume production early 2014. TSMC's phase 6 at Fab 12 in Hsinchu was slated to be TSMC's first 20-nm production site, coming on stream in 2013.

So an early ramping of Fab 14 looks to be an effort to expand 20-nm production capacity and pull it back into 2013. Many observers are tying this to the expectation that TSMC will make the A7 processor for Apple.

TSMC's ability to transition manufacturing of chips from 28-nm to 20-nm bulk CMOS is seen as a key advantage over competitors Samsung and Globalfoundries but on the other hand some observers have said the process will not bring clear performance or power consumption benefits so that many customers would prefer to wait for a FinFET process at 16-nm or 14-nm. But all these processes are present extreme technical complexities that could affect yield and a foundry's ability to supply demand.

Join the premier professional organization for mask makers and mask users!

About the BACUS Group

Founded in 1980 by a group of chrome blank users wanting a single voice to interact with suppliers, BACUS has grown to become the largest and most widely known forum for the exchange of technical information of interest to photomask and reticle makers. BACUS joined SPIE in January of 1991 to expand the exchange of information with mask makers around the world.

The group sponsors an informative monthly meeting and newsletter, BACUS News. The BACUS annual Photomask Technology Symposium covers photomask technology, photomask processes, lithography, materials and resists, phase shift masks, inspection and repair, metrology, and quality and manufacturing management.

Individual Membership Benefits include:

- Subscription to BACUS News (monthly)
- Complimentary Subscription *Semiconductor International* magazine
- Eligibility to hold office on BACUS Steering Committee

www.spie.org/bacushome

Corporate Membership Benefits include:

- Three Voting Members in the SPIE General Membership
- Subscription to BACUS News (monthly)
- One online SPIE Journal Subscription
- Listed as a Corporate Member in the BACUS Monthly Newsletter

www.spie.org/bacushome

Calendar

2013

SPIE Photomask Technology

10-12 September 2013
Monterey Marriott and
Monterey Conference Center
Monterey, California, USA
www.spie.org/pm

Submit late abstracts via the web for consideration by conference chairs.

2014

SPIE Advanced Lithography

23-27 February 2014
San Jose Convention Center
and San Jose Marriott
San Jose, California, USA
www.spie.org/al

SPIE is the international society for optics and photonics, a not-for-profit organization founded in 1955 to advance light-based technologies. The Society serves nearly 225,000 constituents from approximately 150 countries, offering conferences, continuing education, books, journals, and a digital library in support of interdisciplinary information exchange, professional growth, and patent precedent. SPIE provided over $3.2 million in support of education and outreach programs in 2012.

SPIE

International Headquarters
P.O. Box 10, Bellingham, WA 98227-0010 USA
Tel: +1 360 676 3290
Fax: +1 360 647 1445
help@spie.org • www.SPIE.org

Shipping Address
1000 20th St., Bellingham, WA 98225-6705 USA

SPIE Europe
2 Alexandra Gate, Ffordd Pengam, Cardiff,
CF24 2SA, UK
Tel: +44 29 2089 4747
Fax: +44 29 2089 4750
spieeurope@spieeurope.org • www.spieeurope.org

You are invited to submit events of interest for this calendar. Please send to lindad@spie.org; alternatively, email or fax to SPIE.